

Effect of Ca substitution on phase compositions and dielectric properties of $\text{Bi}_2\text{O}_3\text{--ZnO--Nb}_2\text{O}_5$ pyrochlore ceramics

Li-Xia Pang^a, Di Zhou^{b,*}, Hong Wang^b

^aLaboratory of Thin Film Techniques and Optical Test, Xi'an Technological University, Xi'an 710032, China

^bElectronic Materials Research Laboratory & International Center for Dielectric Research, Key Laboratory of the Ministry of Education, Xi'an Jiaotong University, Xi'an 710049, China

Available online 17 October 2012

Abstract

The phase evolution, microstructure and dielectric properties in the Ca^{2+} substituted $\text{Bi}_2\text{O}_3\text{--ZnO--Nb}_2\text{O}_5$ system were studied. The crystalline phases of the $[\text{Bi}_{1.8}(\text{Ca}_x\text{Zn}_{1-x})_{0.2}](\text{Zn}_{0.6}\text{Nb}_{1.4})\text{O}_7$ pyrochlores ($0.0 \leq x \leq 1.0$) depend greatly on the ratio of ionic radius A/B. With the Ca^{2+} substitution for Zn^{2+} in the A site, the crystalline phase transformed from cubic to monoclinic and pure monoclinic phase was obtained for $x \geq 0.5$. As the x value increased from 0.5 to 1.0, the permittivity in the microwave range decreased from 76.4 to 75.0, the quality factor Qf value increased from 1800 to 4700 GHz, and the TCF value shifted from -99 to -147 ppm/ $^\circ\text{C}$.

© 2012 Elsevier Ltd and Techna Group S.r.l. All rights reserved.

Keywords: A. Sintering; C. Dielectric properties; E. Capacitors

1. Introduction

A large number of pyrochlores have been synthesized with an amazing variety of chemical compositions and exploitable properties [1–3]. These include dielectric, ferroelectric, piezoelectric, ferromagnetic, anti-ferromagnetic, high-permittivity properties, catalytic behavior, colossal magneto-resistance (CMR), etc. [4–6]. In 1931, Gaertner et al. [7] described the structure of the ideal oxide pyrochlores. The overall formula of pyrochlore is $\text{A}_2\text{B}_2\text{O}_7$, and it is often written as $\text{A}_2\text{B}_2\text{O}_6\text{O}'$ to distinguish the oxygen atoms in the two different networks $\text{A}_2\text{O}'$ and B_2O_6 . The larger A-cations are 8-fold ($=6+2$) coordinated by six oxygens in puckered rings of the B_2O_6 network plus two O' oxygens above and below in the $\text{A}_2\text{O}'$ network. The structure inherently facilitates non-stoichiometry as the $\text{A}_2\text{O}'$ network can be partially occupied, or in some cases completely absent. In 1970s, bismuth-based pyrochlore compounds of $\text{Bi}_2\text{O}_3\text{--ZnO--Nb}_2\text{O}_5$ (BZN) ternary system for multilayer capacitors were explored in Chinese industry. The general chemical formula of BZN can be written as $\text{Bi}_{3x}\text{Zn}_{2-3x}\text{Zn}_x\text{Nb}_{2-x}\text{O}_7$. For $x=0.5$, the chemical formula

is $\text{Bi}_{1.5}\text{ZnNb}_{1.5}\text{O}_7$ and the system crystallizes in cubic pyrochlore structure (α phase) [8,9]. The ceramic has a microwave permittivity of about 150, a quality factor (Qf) of around 100 GHz, and a temperature coefficient of capacitance (TCC) about -400 ppm/ $^\circ\text{C}$ [8,10]. For $x=2/3$, the chemical formula is $\text{Bi}_2\text{Zn}_{2/3}\text{Nb}_{4/3}\text{O}_7$, and its structure is monoclinic (β phase) [8,11] with a permittivity ~ 80 , a Qf value ~ 3000 GHz, and TCC $\sim +200$ ppm/ $^\circ\text{C}$ [8,12]. When x lies between 0.56 and 0.64, both α and β phase BZN exist in the ceramics and the phase proportion is adjustable by the composition [13]. The high permittivities, relatively low dielectric losses (high quality factor), controllable TCC with the low sintering temperatures (below 1000 $^\circ\text{C}$), and high dielectric tunability with electric field [14] make this system a very appealing candidate for applications in low-firing high-frequency multilayer devices.

In the BZN system, Bi^{3+} prefers to occupy A site due to its large radius (1.17 Å) and Nb^{5+} prefers to occupy B site because of its small radius (0.64 Å), whereas Zn^{2+} is distributed in both A and B sites due to its medium radius (0.74 Å for 6-fold and 0.90 Å for 8-fold) but prefers to enter B site firstly [8]. Previous work [15] reveals that the Ca^{2+} (1.12 Å) substitution for Zn^{2+} in A site of $\text{Bi}_{3x}\text{Zn}_{2-3x}\text{Zn}_x\text{Nb}_{2-x}\text{O}_7$ ($x=0.56\text{--}0.64$) will lead the transformation from α phase to β phase and a pure β phase is

*Corresponding author.

E-mail address: zhoudi1220@gmail.com (D. Zhou).

obtained in $(\text{Bi}_{3-x}\text{Ca}_{2-3x})(\text{Zn}_x\text{Nb}_{2-x})\text{O}_7$ ($x=0.56\text{--}0.64$) system. In this work, the phase evolution in the Ca^{2+} substituted BZN system was studied. The dielectric properties were also investigated.

2. Experimental procedure

Proportionate amounts of reagent-grade starting materials of Bi_2O_3 , ZnO , Nb_2O_5 , and CaCO_3 with high purity were prepared according to the stoichiometric formulation $[\text{Bi}_{1.8}(\text{Ca}_x\text{Zn}_{1-x})_{0.2}](\text{Zn}_{0.6}\text{Nb}_{1.4})\text{O}_7$ ($x=0, 0.2, 0.5, 0.8, 1.0$) compositions. Powders were mixed and ball milled for 4.5 h using a planetary mill (Nanjing Machine Factory, China) by setting the running speed at 150 rpm with zirconia balls (2 mm in diameter) as the milling media. After drying, the mixed oxides were calcined at $750\text{--}850\text{ }^\circ\text{C}$ for 4 h. After crushing and remilling for 5 h, powders were pressed into

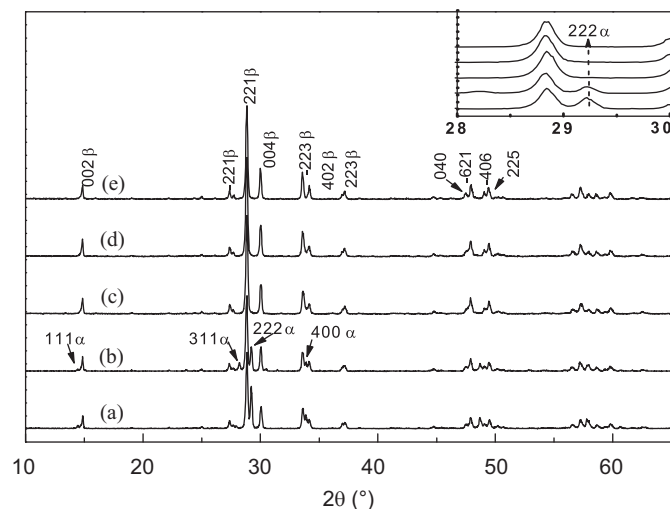


Fig. 1. X-ray diffraction patterns of $[\text{Bi}_{1.8}(\text{Ca}_x\text{Zn}_{1-x})_{0.2}](\text{Zn}_{0.6}\text{Nb}_{1.4})\text{O}_7$ ceramics: (a) $x=0.0$, (b) $x=0.2$, (c) $x=0.5$, (d) $x=0.8$ and (e) $x=1.0$.

Table 1

Relationship between the ratio of ionic radius (A cation to B cation) and crystalline phases in the $\text{Bi}_2\text{O}_3\text{--MO--ZnO--Nb}_2\text{O}_5$ pyrochlores (M=Ca, Sr, Ba, Cd).

Sample	A cation (Å)	B cation (Å)	A/B	Phase
$(\text{Bi}_{1.5}\text{Zn}_{0.5})(\text{Zn}_{0.5}\text{Nb}_{1.5})\text{O}_7$ [8,9]	2.205	1.33	1.658	α
$\text{Bi}_2\text{Zn}_{2/3}\text{Nb}_{4/3}\text{O}_7$ [8,11]	2.34	1.347	1.738	β
$(\text{Bi}_{3-x}\text{Zn}_{2-3x})(\text{Zn}_x\text{Nb}_{2-x})\text{O}_7$ [16]	$x=0.56$	2.25	1.336	$\alpha+\beta$
	$x=0.64$	2.32	1.344	$\alpha+\beta$
$(\text{Bi}_{3-x}\text{Ca}_{2-3x})(\text{Zn}_x\text{Nb}_{2-x})\text{O}_7$ [15]	$x=0.56$	2.32	1.336	β
	$x=0.64$	2.34	1.344	β
$[\text{Bi}_{1.8}(\text{Ca}_x\text{Zn}_{1-x})_{0.2}](\text{Zn}_{0.6}\text{Nb}_{1.4})\text{O}_7$	$x=0.0$	2.29	1.34	$\alpha+\beta$
	$x=0.2$	2.29	1.34	$\alpha+\beta$
	$x=0.5$	2.31	1.34	β
	$x=0.8$	2.32	1.34	β
	$x=1.0$	2.33	1.34	β
$(\text{Bi}_{1.92}\text{M}_{0.08})(\text{Zn}_{0.64}\text{Nb}_{1.36})\text{O}_7$ [17]	M=Ca	2.34	1.344	β
	M=Sr	2.347	1.344	β
	M=Cd	2.334	1.344	β
	M=Ba	2.36	1.344	$\beta+\text{BBN}$

BBN, $\text{BaBi}_2\text{NbO}_9$.

pellets and cylinders (10 mm in diameter and 5 mm in height) using a steel die under a uniaxial pressure of 200 MPa with PVA binder addition. Samples were sintered in air at temperatures from 930 to 1020 $^\circ\text{C}$ for 2 h.

The crystalline structures of samples (ground powders) were investigated using X-ray diffraction (XRD) with $\text{Cu K}\alpha$ radiation (Rigaku D/MAX-2400 X-ray diffractometry, Tokyo, Japan). The apparent densities were measured by Archimede's method. Micro-structural study of the sample was conducted via scanning electron microscopy (SEM) (JSM-6460, JEOL, Tokyo, Japan). The capacitances versus frequency were measured using HP 4284A impedance analyzer. The dielectric properties were measured at microwave frequency by the TE_{018} shielded cavity method with a network analyzer (8720ES, Agilent, Palo Alto, CA) and a temperature chamber (Delta 9023, Delta Design, Poway, CA). The temperature coefficient of resonant frequency (TCF) was calculated by the following formula:

$$\text{TCF} = \frac{f_{85} - f_{25}}{f_{25}(85 - 25)} \times 10^6 \text{ (ppm/}^\circ\text{C)} \quad (1)$$

where f_{85} and f_{25} were the TE_{018} resonant frequencies at 85 and 25 $^\circ\text{C}$, respectively.

3. Results and discussion

Fig. 1 shows the XRD patterns of the $[\text{Bi}_{1.8}(\text{Ca}_x\text{Zn}_{1-x})_{0.2}](\text{Zn}_{0.6}\text{Nb}_{1.4})\text{O}_7$ ($0 \leq x \leq 1.0$) powdered ceramics. As seen from Fig. 1, both α and β phases were observed in sample with $x=0.0$. With the Ca^{2+} substitution for Zn^{2+} in the A site, the $\alpha \rightarrow \beta$ phase transformation occurred and pure β phase was obtained when $x \geq 0.5$. The relationship between the ratio of ionic radius (A cation to B cation) and crystalline phases in the $\text{Bi}_2\text{O}_3\text{--MO--ZnO--Nb}_2\text{O}_5$ pyrochlores is shown in Table 1. The crystalline phases of $\text{Bi}_2\text{O}_3\text{--MO--ZnO--Nb}_2\text{O}_5$ pyrochlore depend greatly on the ratio of ionic radius A/B. As seen from Table 1, the $\text{Bi}_2\text{O}_3\text{--MO--ZnO--Nb}_2\text{O}_5$

pyrochlore crystallizes as a pure α phase when the ratio of ionic radius A/B is less than 1.687, and pure β phase is obtained when the A/B is higher than 1.725 but less than 1.756. For $1.687 \leq A/B \leq 1.725$, both α and β phases are formed.

In this work, pure β phase was formed in the $[\text{Bi}_{1.8}(\text{Ca}_x\text{Zn}_{1-x})_{0.2}](\text{Zn}_{0.6}\text{Nb}_{1.4})\text{O}_7$ sample for $x=0.5$, in which the A/B was 1.722, less than 1.725. This result means that the phase composition was also influenced by other factors, such as sintering temperature [16], when the A/B was near to 1.725. In the $\text{Bi}_2\text{O}_3\text{--MO--ZnO--Nb}_2\text{O}_5$ pyrochlores, NbO_6 and ZnO_6 octahedra with shared vertices form a three-dimensional network resulting in large cavities which contain the O' and A site atoms in an $\text{A}_2\text{O}'$ tetrahedral net. When the ionic radius of A cation is smaller than the size of the cavity which is formed by the BO_6 octahedra, cubic pyrochlore phase (α phase) is obtained with the A-cation displacement toward a pair of the framework O atoms [18]. When the ionic radius of A cation is large enough, the cubic pyrochlore phase cannot be maintained and it turns to the monoclinic phase (β phase). Thus, the Ca^{2+} substitution for Zn^{2+} in the A site results in the phase transformation from α phase to β phase and pure β phase is obtained when $x \geq 0.5$.

SEM micrographs of fractured surfaces and as-fired surfaces demonstrate the microstructure of the $[\text{Bi}_{1.8}(\text{Ca}_x\text{Zn}_{1-x})_{0.2}](\text{Zn}_{0.6}\text{Nb}_{1.4})\text{O}_7$ ceramics ($0 \leq x \leq 1.0$) sintered

at 950 °C, as shown in Fig. 2(a–e). Dense and homogeneous microstructures could be revealed in all compositions with the grain size between 1–3 μm . Because of the similar morphology and composition, it is difficult to distinguish between the grains of α phase and β phase in the SEM micrographs and BES imaging (as shown in Fig. 2).

To determine the effect of Ca^{2+} substitution on the dielectric properties, the dielectric spectroscopy of the $[\text{Bi}_{1.8}(\text{Ca}_x\text{Zn}_{1-x})_{0.2}](\text{Zn}_{0.6}\text{Nb}_{1.4})\text{O}_7$ ceramics were measured in the frequency range of 100 Hz–1 MHz, as shown in Fig. 3. The permittivities of all samples were kept stable in the frequency range of 100 Hz–1 MHz. On the other hand, when $x \leq 0.5$, the permittivity decreased greatly from about 140 to 90 with the Ca^{2+} substitution, which was due to the phase transformation from α phase to β phase.

When x value increased from 0.5 to 1.0, the permittivity decreased slightly from 90 to about 80 (at 1 MHz). Table 2 presents the microwave dielectric properties of the $[\text{Bi}_{1.8}(\text{Ca}_x\text{Zn}_{1-x})_{0.2}](\text{Zn}_{0.6}\text{Nb}_{1.4})\text{O}_7$ ceramics ($0.5 \leq x \leq 1.0$). As the x value increased from 0.5 to 1.0, the permittivity in the microwave range decreased slightly from 76.4 to 75.0, the quality factor Qf value increased greatly from 1800 to 4700 GHz, and the TCF value shifted from -99 to -147 ppm/°C.

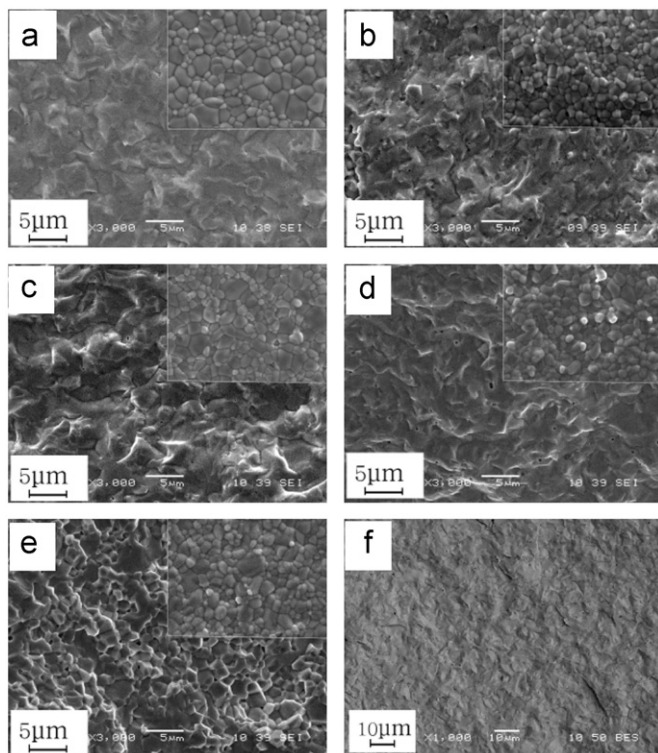


Fig. 2. Scanning electron microscopy of the fractured surface and as-fired surface (the top right corner) of $[\text{Bi}_{1.8}(\text{Ca}_x\text{Zn}_{1-x})_{0.2}](\text{Zn}_{0.6}\text{Nb}_{1.4})\text{O}_7$ ceramics sintered at 950 °C for 2 h: (a) $x=0.0$, (b) $x=0.2$, (c) $x=0.5$, (d) $x=0.8$, (e) $x=1.0$, and (f) backscattered electron imaging of the fractured surface of $x=0.0$ sample.

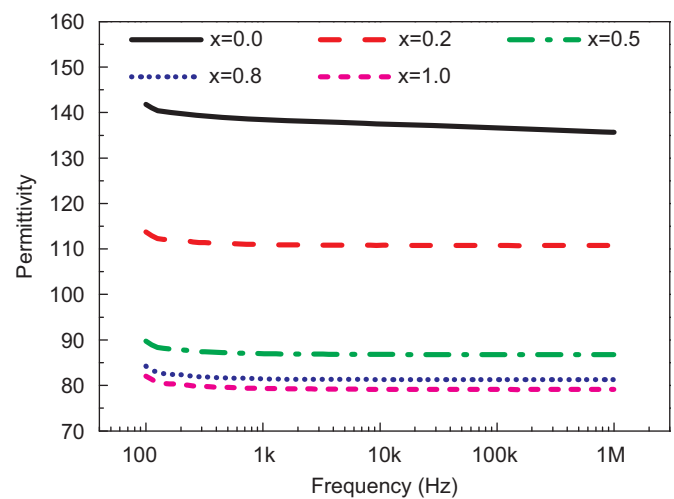


Fig. 3. Dielectric spectroscopy of the $[\text{Bi}_{1.8}(\text{Ca}_x\text{Zn}_{1-x})_{0.2}](\text{Zn}_{0.6}\text{Nb}_{1.4})\text{O}_7$ ceramics.

Table 2

Microwave dielectric properties of the $[\text{Bi}_{1.8}(\text{Ca}_x\text{Zn}_{1-x})_{0.2}](\text{Zn}_{0.6}\text{Nb}_{1.4})\text{O}_7$ ceramics.

Sample	Permittivity	Frequency (GHz)	Qf (GHz)	TCF (ppm/°C)
$x=0.5$	76.4	4.07	1800	-99
$x=0.8$	75.8	4.09	4100	-121
$x=1.0$	75.0	4.15	4700	-147

4. Conclusions

The $[\text{Bi}_{1.8}(\text{Ca}_x\text{Zn}_{1-x})_{0.2}](\text{Zn}_{0.6}\text{Nb}_{1.4})\text{O}_7$ ($0.0 \leq x \leq 1.0$) ceramics were fabricated by the conventional solid state reaction method. All the samples could be well densified after being sintered at $900 \sim 1000$ °C for 2 h. The crystalline phases of $\text{Bi}_2\text{O}_3\text{--MO--ZnO--Nb}_2\text{O}_5$ pyrochlore depend greatly on the ratio of ionic radius A/B. In the $[\text{Bi}_{1.8}(\text{Ca}_x\text{Zn}_{1-x})_{0.2}](\text{Zn}_{0.6}\text{Nb}_{1.4})\text{O}_7$ ($0.0 \leq x \leq 1.0$) system, with the Ca^{2+} substitution for Zn^{2+} in the A site, the phase transformation from α to β occurred and pure β phase was obtained for $x \geq 0.5$. As the x value increased from 0.5 to 1.0, the permittivity in the microwave range decreased from 76.4 to 75.0, the quality factor Qf value increased from 1800 to 4700 GHz, and the TCF value shifted from -99 to -147 ppm/°C.

Acknowledgments

This work was supported by the NSFC projects of China (51202182, 51202178), Foundation of Shaanxi Educational Committee (12JK0432), Fundamental Research Funds for the Central University and the headmaster foundation of Xi'an Technological University (XAGDXJJ1001).

References

- [1] W.B. Yuan, Y.F. Hua, Z. Guang, New pyrochlore-type compound containing $\text{Bi}_2\text{O}_3\text{--MgO--Nb}_2\text{O}_5$, *Advanced Ceramics* 7 (1984) 239–245.
- [2] M.W. Lufaso, T.A. Vanderah, I.M. Pazos, I. Levin, R.S. Roth, J.C. Nino, V. Provenzano, P.K. Schenck, Phase formation, crystal chemistry, and properties in the system $\text{Bi}_2\text{O}_3\text{--Fe}_2\text{O}_3\text{--Nb}_2\text{O}_5$, *Journal of Solid State Chemistry* 179 (2006) 3900–3910.
- [3] T.A. Vanderah, M.W. Lufaso, A.U. Adler, I. Levin, J.C. Nino, V. Provenzano, P.K. Schenck, Subsolidus phase equilibria and properties in the system $\text{Bi}_2\text{O}_3\text{:Mn}_2\text{O}_3 \pm x$, *Journal of Solid State Chemistry* 179 (2006) 3467–3477.
- [4] D. Zhou, H. Wang, X. Yao, L.X. Pang, Sintering behavior and microwave dielectric properties of $\text{Bi}_2\text{O}_3\text{--ZnO--Nb}_2\text{O}_5$ -based ceramics sintered under air and N_2 atmosphere, *Ceramics International* 34 (2008) 901–904.
- [5] T.A. Vanderah, I. Levin, An unexpected crystal-chemical principle for the pyrochlore structure, *European Journal of Inorganic Chemistry* 2005 (2005) 2895–2901.
- [6] D. Zhou, H. Wang, X. Yao, Layered complex structures of $\text{Bi}_2(\text{Zn}_{2/3}\text{Nb}_{4/3})\text{O}_7$ and BiNbO_4 dielectric ceramics, *Materials Chemistry and Physics* 105 (2007) 151–153.
- [7] H. Von Gaertner, Die kristallstrukturen von loparite und pyrochlore, *Neues Jahrbuch für Mineralogie, Geologie und Palaeontologie* 61 (1930) 1–30.
- [8] X.L. Wang, H. Wang, X. Yao, Structures, phase transformations, and dielectric properties of pyrochlores containing bismuth, *Journal of the American Ceramic Society* 80 (1997) 2745–2748.
- [9] I. Levin, T.G. Amos, J.C. Nino, T.A. Vanderah, C.A. Randall, M.T. Lanagan, Structural study of an unusual cubic pyrochlore $\text{Bi}_{1.5}\text{Zn}_{0.92}\text{Nb}_{1.5}\text{O}_{6.92}$, *Journal of Solid State Chemistry* 168 (2002) 69–75.
- [10] J.C. Nino, M.T. Lanagan, C.A. Randall, Dielectric relaxation in $\text{Bi}_2\text{O}_3\text{--ZnO--Nb}_2\text{O}_5$ cubic pyrochlore, *Journal of Applied Physics* 89 (2001) 4512–4516.
- [11] I. Levin, T.G. Amos, J.C. Nino, T.A. Vanderah, I.M. Reaney, C.A. Randall, M.T. Lanagan, Crystal structure of the compound $\text{Bi}_2\text{Zn}_{2/3}\text{Nb}_{4/3}\text{O}_7$, *Journal of Materials Research* 17 (2002) 1406–1411.
- [12] D. Liu, Y. Liu, S. Huang, X. Yao, Phase Structure and dielectric properties of $\text{Bi}_2\text{O}_3\text{--ZnO--Nb}_2\text{O}_5$ -based dielectric ceramics, *Journal of the American Ceramic Society* 76 (1993) 2129–2132.
- [13] S.L. Swartz, T.R. Shrout, Ceramic composition for BZN dielectric resonator, U. S. Patent No. 5449652 (1995).
- [14] W. Ren, S. Trolier-McKinstry, C.A. Randall, T.R. Shrout, Bismuth zinc niobate pyrochlore dielectric thin films for capacitive applications, *Journal of Applied Physics* 89 (2001) 767–774.
- [15] M.L. Zhang, H. Wang, X. Yao, Effect of Ca substitution on structure and dielectric properties of bismuth-based microwave ceramics, *Journal of Electroceramics* 21 (2008) 461–464.
- [16] H. Wang, X.L. Wang, X. Yao, Phase equilibrium in $\text{Bi}_2\text{O}_3\text{--ZnO--Nb}_2\text{O}_5$ system, *Ferroelectrics* 195 (1997) 19–22.
- [17] H. Wang, S. Kamba, M.L. Zhang, X. Yao, S. Denisov, F. Kadlec, J. Petzelt, Microwave and infrared dielectric response of monoclinic bismuth zinc niobate based pyrochlore ceramics with ion substitution in A site, *Journal of Applied Physics* 100 (2006) 034109.
- [18] V. Krayzman, I. Levin, J.C. Woicik, Local structure of displacive-disordered pyrochlore dielectrics, *Chemistry of Materials* 19 (2007) 932–936.